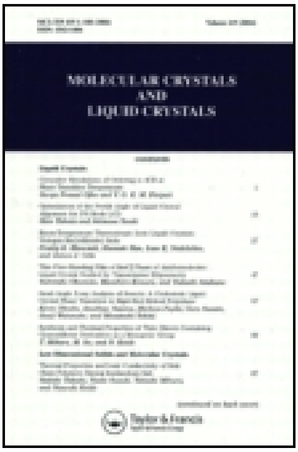

Molecular Crystals and Liquid Crystals
Publication details, including instructions for authors and subscription information:
http://www.tandfonline.com/loi/gmcl20

Photonic Band Gap Fibers with Novel Chiral Nematic and Low-Birefringence Nematic Liquid Crystals

Marzena M. Tefelska [a], Miłosz S. Chychłowski [a], Tomasz R. Woliński [a], Roman Dąbrowski [b], Wojciech Rejmer [b], Edward Nowinowski-Kruszelnicki [b] & Paweł Mergo [c]

[a] Faculty of Physics, Warsaw University of Technology, Poland

[b] Military University of Technology, Warsaw, Poland

[c] Maria Curie Skłodowska University, Lublin, Poland

Version of record first published: 18 Apr 2012.

To cite this article: Marzena M. Tefelska, Miłosz S. Chychłowski, Tomasz R. Woliński, Roman Dąbrowski, Wojciech Rejmer, Edward Nowinowski-Kruszelnicki & Paweł Mergo (2012): Photonic Band Gap Fibers with Novel Chiral Nematic and Low-Birefringence Nematic Liquid Crystals, Molecular Crystals and Liquid Crystals, 558:1, 184-193

To link to this article: http://dx.doi.org/10.1080/15421406.2011.654187

Mol. Cryst. Liq. Cryst., Vol. 558: pp. 184–193, 2012

ISSN: 1542-1406 print/1563-5287 online
DOI: 10.1080/15421406.2011.654187

Photonic Band Gap Fibers with Novel Chiral Nematic and Low-Birefringence Nematic Liquid Crystals

MARZENA M. TEFELSKA,[1,*] MIŁOSZ S. CHYCHŁOWSKI,[1] TOMASZ R. WOLIŃSKI,[1] ROMAN DĄBROWSKI,[2] WOJCIECH REJMER,[2] EDWARD NOWINOWSKI-KRUSZELNICKI,[2] AND PAWEŁ MERGO[3]

[1]Faculty of Physics, Warsaw University of Technology, Poland
[2]Military University of Technology, Warsaw, Poland
[3]Maria Curie Skłodowska University, Lublin, Poland

In this paper the latest experimental results of a novel PW600 chiral nematic liquid crystal with significantly reduced temperature sensitivity of the selective Bragg reflection are presented. The PW600 liquid crystal was used to fill prototype photonic crystal fibers with 3, 5, 6 and 8 rings of the holes manufactured by MCSU, Lublin and temperature—induced photonic band gap shifts have been observed. Additionally, experimental results with a new low-birefringence nematic liquid crystal 1800B are presented. The results obtained suggest great potential of the liquid crystals filled photonic crystal fibers for optical fiber attenuators and modulators.

Keywords Chiral nematic; helicoidal pitch; photonic crystal fibers

1. Introduction

Over the past decade, photonic crystal fibers (PCF) have become the subject of an increasing research interest. Particular attention has been focused on the possibility of filling the air holes of photonic crystal fibers with liquid crystals [1] due to their high sensitivity to temperature and external physical fields. Thermally, electrically and optically tunable micro-structured fibers filled with liquid crystals have been recently reported [2–8].

Propagation of light in photonic crystals fibers can be guided by two different mechanisms: index guiding (also known as the modified Total Internal Reflection–mTIR) and the photonic band gap effect (PBG). Light propagation can be easily modified in photonic crystal fibers either by a special fiber structure design or filling these microstructured fibers with various materials of particular properties. Liquid crystals (LC) are very interesting substances to infiltrate photonic crystal fibers due to their optical properties that strongly depend on thermal, electric, magnetic and even optical fields. Hence the mechanism of propagating light in these structures can be changed when temperature or electric field

*Address correspondence to M. M. Tefelska. Faculty of Physics, Warsaw University of Technology, Poland. E-mail: martef@if.pw.edu.pl

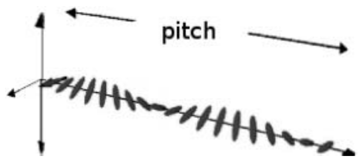

Figure 1. Pitch of the helical CNLC structure.

is applied. The majority of up-to-date research activities have been focused on photonic crystal fibers filled with nematic liquid crystals.

Chiral nematic liquid crystals (CNLCs) seem to be novel and interesting materials to infiltrate PCFs. The chiral nematic phase exhibits spatial twisting of molecules perpendicular to the director. Chirality induces a finite azimuthal twist from one layer to another, producing helicoidal twisting of the molecular axis along the layer normal.

An important characteristic of the CNLC (also known as cholesteric LC) mesophase its helicoidal pitch p, defined as a distance it takes for the director to rotate one full turn in the helix (Fig. 1). The helical structure of the chiral nematic phase has the ability to selectively reflect light of wavelengths equal to the pitch length, so the special wavelength of light spectrum will be reflected when the pitch is equal to the corresponding wavelength of light in the visible spectrum.

The helicoidal pitch is usually temperature-dependent and it can also be affected by the boundary conditions when the chiral nematic liquid crystal is placed between two surfaces.

2. Materials and Experimental Setup

In this experiment novel LCs materials: the PW600 (also known as MTW1 [8]) chiral nematic LC and a low birefringence 1800B mixture synthesized at the Military University of Technology (Warsaw, Poland) were used. The chiral nematic liquid crystal composed of alkylcyclohexyl and bicyclohexylbenzene nitryles and isothiocyanates and an optically active dopant (OAD1) (9.4% weight content) responsible for molecular structure winding. The chemical structure of the OAD1 is shown in Fig. 2.

The PW600 LC has chiral nematic-isotropic liquid phase transition (N*-Iso) at 83.2°C, and it is characterized by significantly reduced temperature sensitivity of the selective Bragg reflection (Fig. 3(a)). Its helical pitch ∼400 nm at room temperature (22°C) was measured by the Grandjean-Cano method. Figure 3(b) shows the Grandjean-Cano stripes that were observed under the polarizing microscope. Since the mean refractive index of the PW600 LC is higher than the refractive index of the silica glass, the effective LC-infiltrate PCFs can propagate light only due to the photonic band gap mechanism.

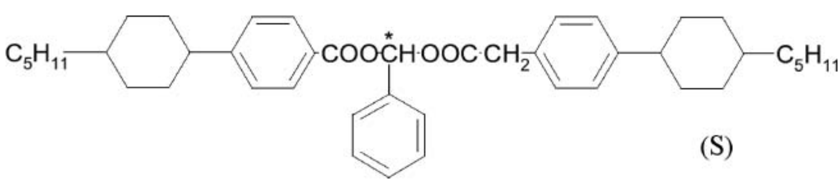

Figure 2. Right-handed optically active dopant OAD 1 with helicoidal twisting power HTP = 67.2 μm^{-1}.

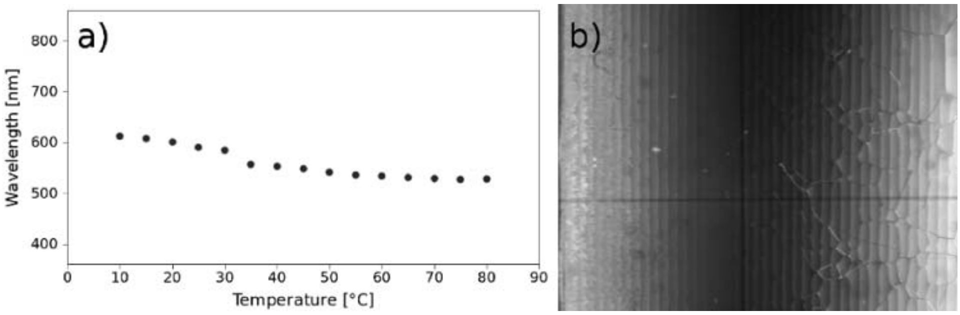

Figure 3. a) A selective Bragg reflection for the PW600 chiral nematic LC upon temperature, b) Grandjean-Cano stripes.

A new low-birefringence 1800B LC is a modification of the well-known 1550 low-birefringence nematic mixture described elsewhere [9]. The chemical structure of the 1800B LC mixture is shown in Fig. 4(a). It is characterized by phase transitions temperatures: S_B10N71.5Iso and has a wide temperature range of the nematic phase (20–71.5°C) in which its ordinary refractive index n_o is below the refractive index of the fused silica $n_{silica} = 1.458$ (at $\lambda = 588$ nm) while its extraordinary index is still higher than n_{silica} (Fig. 4(b)). Birefringence of the 1800B LC at 20°C is very low and equals: $\Delta n = 0.0596$.

In experimental photonic crystal fibers manufactured at the Maria Curie Skłodowska University (UMCS, Lublin, Poland) with 3 (Fig. 5(a)), 5 (Fig. 5(b)), 6 (Fig. 5(c)) and 8 (Fig. 5(d)) rings of the holes were filled with the PW600 chiral nematic LC. In case of PCF with 5 rings of the holes the 1800B nematic mixture was also applied.

As a light source, a halogen lamp (Mikropack Halogen LightSource HL-2000) was used. As a light intensity detector, we used the HR4000 Ocean Optics spectrometer. Temperature was controlled by the Peltier module (Fig. 6).

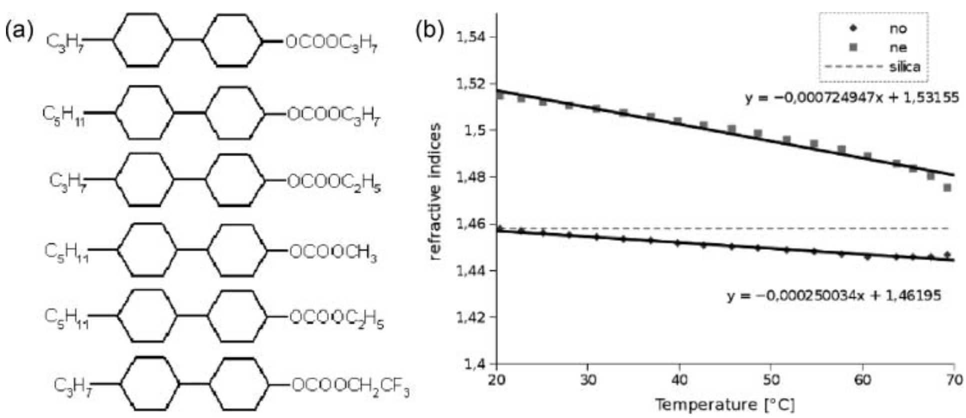

Figure 4. a) Chemical structure of the 1800B mixture, b) refractive indices as a function of temperature for 1800B liquid crystal.

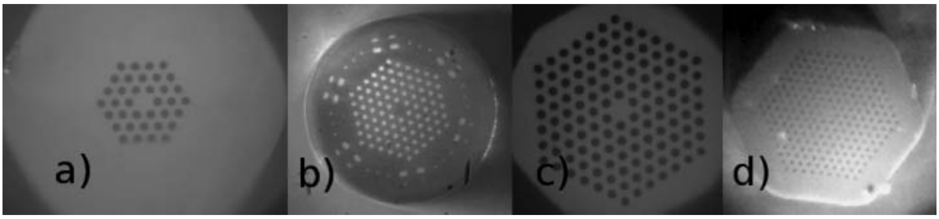

Figure 5. Cross-sections of photonic crystal fibers with a) 3 b) 5, c) 6 and d) 8 rings of holes, manufactured at the (MCSU, Lublin, Poland).

3. Experimental Results

3.1. PW600 in Cells and Capillaries

Preliminary studies with the PW600 chiral nematic liquid crystal were made in liquid crystal cells with a thickness of 20 μm, coated with a planar orienting layer (Fig. 7(a)). Figure 7(b) presents myelin filaments of chiral nematic liquid crystal. The value of the threshold electric field (1) was about 21 V/μm (for 415V at frequency 500 Hz) and this caused helical structure unwinding. At the time of helical structure unwinding a transition from the opaque state of a liquid crystal cell to transparent was observed. The LC cell filled with a PW600 chiral nematic is presented in Fig. 8 (pictures were made by the LSCM Nikon Eclipse Ti (A1) confocal microscope, at the Faculty of Biology, University of Warsaw). In this picture the myelin filaments of a chiral nematic liquid crystal are visible. The LC cell was subjected to an external electric field (Fig. 9) above the threshold value of the N*->N transition (helix unwinding).

$$E_c = \frac{\pi^2}{P} \cdot \sqrt{\frac{K_{22}}{\varepsilon_0 \cdot \Delta\varepsilon}} \tag{1}$$

where

E_c—electric field intensity
K_{22}—Frank elastic constant, twist deformation
ε_0—electric permittivity in vacuum
$\Delta\varepsilon$—dielectric anisotropy
P—helicoidal pitch

The induced electric field forces perpendicular orientation to the cell surface in the helix groups of molecules of chiral nematic liquid crystal. The twisted texture causes the opaque state of an LC cell. The opaque state is permanent despite of no electric field applied.

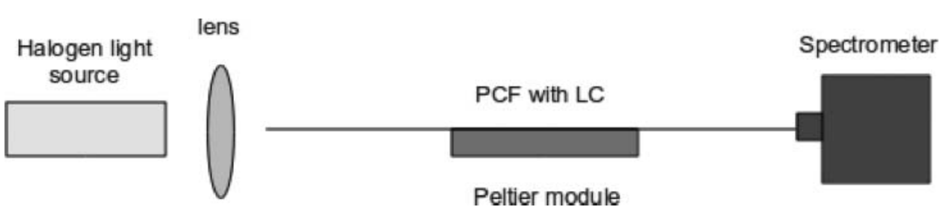

Figure 6. Experimental setup.

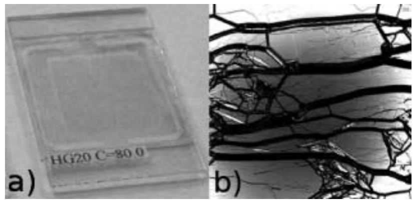

Figure 7. a) LC cell filled with chiral nematic PW600. b) Myelin filaments of chiral nematic liquid crystal. The picture was taken under polarization microscope.

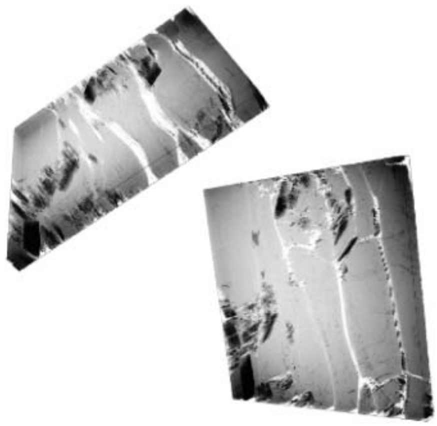

Figure 8. LC cell filled with chiral nematic PW600 without any orientation. Pictures were taken by LSCM Nikon Eclipse Ti (A1), 40× lens confocal microscope, Faculty of Biology, University of Warsaw.

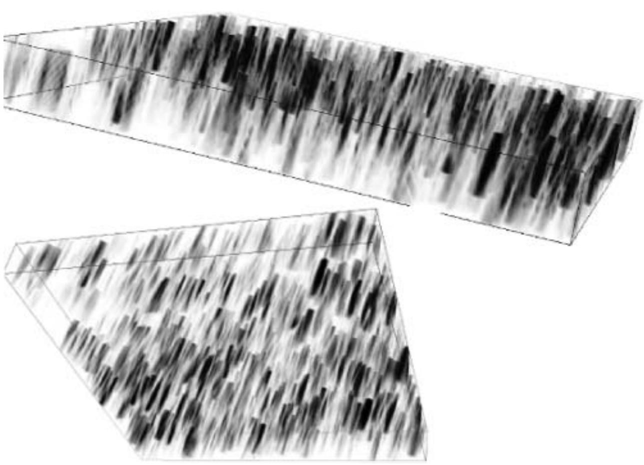

Figure 9. Liquid crystal cell with chiral nematic PW600, exhibiting long lasting memory effect. An external electric field was initially applied and then removed. Pictures were taken by the LSCM Nikon Eclipse Ti (A1), 40× lens confocal microscope, Faculty of Biology, University of Warsaw.

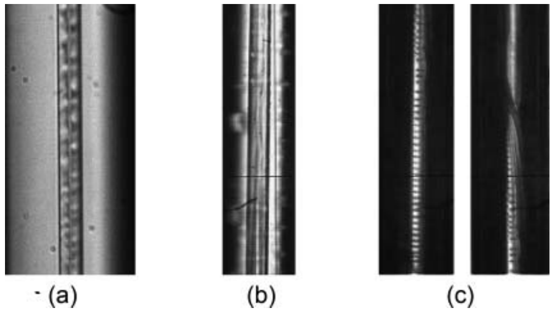

Figure 10. Capillaries filled with PW600 with a internal diameter of a) 10 μm, b) 25 μm and c) 128 μm in temperature of 25°C. Pictures were taken from polarization microscope with 20× lens.

The helical structure of chiral nematic liquid crystal is presented in Fig. 9.

The arrangement of chiral nematic molecules in a capillary is totally different than in the cell due to a much more complicated character of boundary conditions and its cylindrical structure [10,11]. Figure 10 shows the pictures of capillaries filled with LC PW600 without any orienting layer and characterized by internal diameters: 10 μm (Fig. 10(a)), 25 μm (Fig. 10(b)) and 128 μm (Fig. 10(c)) respectively. It can be assumed that the PW600 chiral nematic LC helix is parallel to the capillary long axis. However this arrangement is not uniform, there are some disturbances and also defects resulting from the internal structure of a capillary or a sudden temperature change. The arrangement is strongly dependent on the internal diameter of a capillary and also the type of LC infiltration method.

3.2. Experimental Results in Photonic Liquid Crystal Fibers

The photonic crystal fiber with 3 rings of holes (40 cm of length) was filled with a PW600 LC mixture on the length of 2.7 cm. We have observed PBGs that moved towards shorter wavelengths with increasing temperature (Fig. 11(a)).

The applied electric field was too small to observe helical unwinding and attenuation was increasing while the electric field was applied for the whole range (Fig. 11(b)). For a

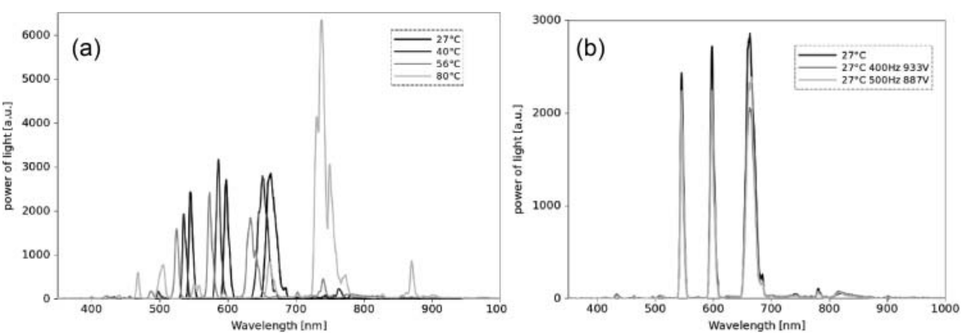

Figure 11. Photonic band gaps tuning by a) temperature and b) influence of electric field for propagating light in photonic crystal fiber with 3 rings of holes filled with PW600 LC.

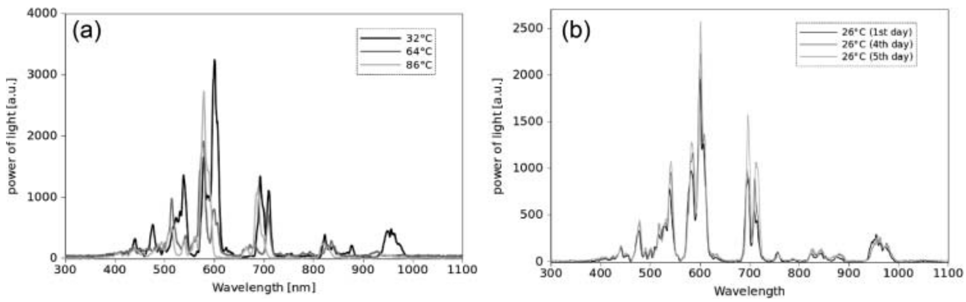

Figure 12. Photonic band gaps shift a) by change of temperature b) time stabilization of propagating light in photonic crystal fiber with 5 rings of holes filled with LC PW600.

photonic crystal fiber with 5 rings of holes (with about 40 cm long) filled with LC PW600 (infiltration length about 2.7 cm) PBGs moving under the influence of temperature were observed (Fig. 12(a)). We checked the long-term stability after ~5 days and observed that the spectrum remained unchanged (Fig. 12(b)).

A photonic crystal fiber with 6 rings of holes was filled with the PW600 mixture. When the temperature was decreasing, the photonic band gaps shifted into the longer wavelength (red shift) (Fig. 13(a)) but when it was increasing, the photonic band gaps shifted into the shorter wavelength (blue shift) (Fig. 13(b)). This is in contrast to well-known 6CHBT or 5CB nematic LCs. Temperature induced wavelength shift $\frac{\Delta\lambda}{\Delta T}$ is about 2 nm/°C. For this configuration the average attenuation of PLCF is at the level ~5.5 dB/cm.

For photonic liquid crystal fiber with 8 rings of holes part of propagating light ~450 nm is emitted out of the core and stay on the boundary of the cladding fiber (Fig. 14). The remaining amount of light with a small fraction of the light was propagating in the core. This effect was repeatable.

The PCF used in the next experiment was ~90 cm long with 5 rings of holes infiltrated with 1800B LC (section of ~3 cm). This fiber has low attenuation and the diameter of about 125 um. The temperature range was changing from 21°C to 71°C by using the Peltier module. The intensity of output light increased when the temperature was increased, as shown in Fig. 15.

In Fig. 16 the operating wavelength depends on temperature and we observed a significant increase in the output power while the temperature rose from 20°C to 65°C. For

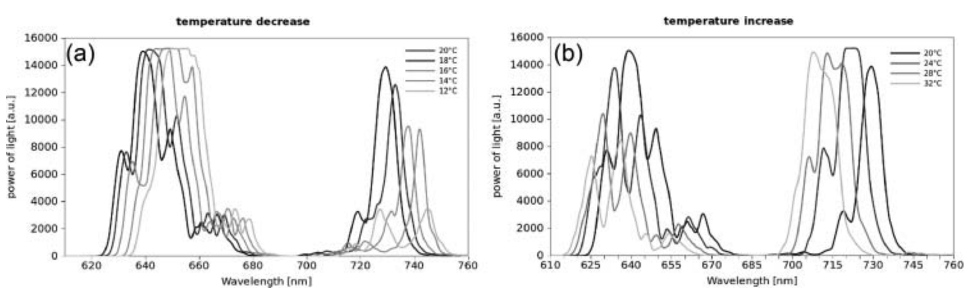

Figure 13. Photonic band gaps shift by change of temperature for photonic crystal fiber with 6 rings of holes filled with PW600, a) red shift, b) blue shift.

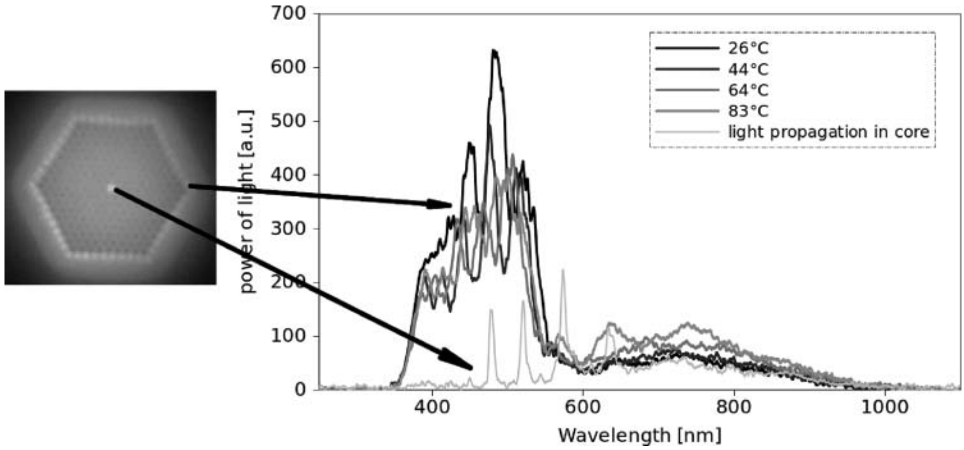

Figure 14. Photonic band gaps tuning and emitted shorter wavelength to fiber cladding, 8 rings of holes filled with PW600.

70.7°C, close to the nematic-isotropic phase transition of an LC, the output power rapidly decreased. In a photonic crystal fiber filled with the 1800B mixture, the light propagation is guided by the modified Total Internal Reflection mechanism, which is characterized by much smaller attenuation (~0.35dB/cm). If the refractive index of an infiltrated material is smaller (if the contrast between the coefficients of refraction of the core and cladding is stronger), the light is better guided. Hence, the type of the PLCF can be used as a fiber with a wide range of tunable attenuation.

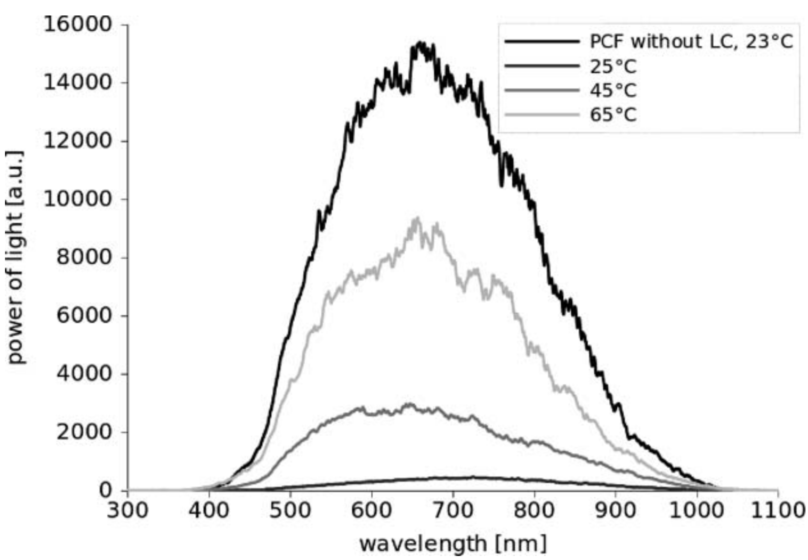

Figure 15. Transmission spectra for PCF infiltrated with LC 1800B under influence of temperature.

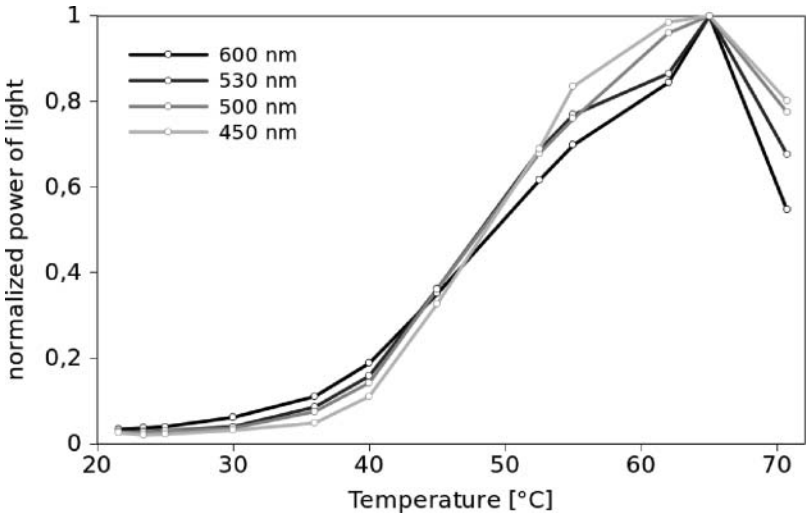

Figure 16. Normalized optical power for selected wavelengths in function of temperature, 5 rings of holes filled with 1800B LC.

4. Conclusions

Photonic crystal fibers filled with various substances can be used as all-in-fiber tunable devices. In this paper, the propagation effects in a PCF filled with a chiral nematic LC and the 1800B mixture have been demonstrated.

The PCF with 6 rings of holes filled with the PW600 could be used as an optical filter because of its photonic band gaps tuning ability. The configuration of a PCF with 5 rings of holes filled with the 1800B shows the possibility of attenuation tuning in the index guiding regime controlled by temperature changes. Consequently, this property may be used to propose a fiber-optic attenuator.

It is believed that through the confocal microscope measurement method it will be possible to determine the helix pitch, choosing appropriate parameters as a pitch of scanning sample, image resolution, depth of scanning. It is possible also that analogous measurement for capillaries filled with liquid crystals will clearly define molecules orientation.

Acknowledgment

The work was supported by the Polish National Science Centre under the grant N507 303040 and by the MISTRZ Programme of the Polish Science Foundation.

The authors acknowledge dr Anna Łasińska for 3D pictures of chiral nematic in an LC cell were made by the LSCM Nikon Eclipse Ti (A1) confocal microscope in the Confocal Microscopy Laboratory at the Faculty of Biology, University of Warsaw.

References

[1] Larsen, T. T., Bjarklev, A., Hermann, D. S., & Broeng, J. (2003). *Opt. Express*, *11*, 2589–2596.
[2] Woliński, T. R., Czapla, A., Ertman, S., Tefelska, M., Domański, A. W., Nowinowski-Kruszelnicki, E., & Dąbrowski, R. (2007). *Optical and Quantum Electronics*, *39*, 1021–1032.

[3] Ertman, S., Czapla, A., Woliński, T. R., Nasiłowski, T., Thienpont, H., Nowinowski-Kruszelnicki, E., & Dąbrowski, R. (2009). *Opto-Electronics Review*, *17*(2), 150–155.
[4] Alkeskojld, T. T., Bjarklev, L. A., Hermann, D. S., Anawati, Broeng, J., Li, J., & Wu, S.T. (2004). *Opt. Express*, *12*, 5857–5871.
[5] Du, F., Lu, Y. Q., & Wu, S. T. (2004). *Appl. Phys. Lett.*, *85*, 2181–2183.
[6] Woliński, T. R., Szaniawska, K., Bondarczuk, K., Lesiak, P., Domański, A. W., Dąbrowski, R., Nowinowski-Kruszelnicki, E., & Wójcik, J. (2005). *Opto-Electronics Review*, *13*(2), 177–182.
[7] Wolinski, T. R., Szaniawska, K., Ertman, S., Lesiak, P., Domanski, A. W., Dabrowski, R., Nowinowski-Kruszelnicki, E., & Wojcik, J. (2006). *Meas. Sci. Technol.*, *17*, 985–991.
[8] Tefelska, M. M., Woliński, T. R., Dąbrowski, R., & Wójcik, J. (2010). *Photonics Letters of Poland*, *2*(1), 28–30.
[9] Dąbrowski, R., Dziaduszek, J., Stolarz, Z., & Kędzierski, J. (2005). *J. Opt. Technol.*, *72*, 662–667.
[10] Kitzerow, H. S., Liu, B., Xu, F., & Crooker, P. P. (1996). *Physical Review E*, *54*(1), 568–575.
[11] Ambrozic, M., & Zumer, S. (1996). *Physical Review E*, *54*(5), 5187–5197.